Journal of Luminescence 201 (2018) 143–147

Contents lists available at ScienceDirect

Journal of Luminescence

journal homepage: www.elsevier.com/locate/jlumin

Dual effects of Nd^{3+} in Nd^{3+}/Ho^{3+}:$CaLaGa_3O_7$ crystal on 2.86 μm emission

Yunyun Liu[a,b], Mingyuan Hu[a,b], Yan Wang[a,*], Zhenyu You[a], Jianfu Li[a], Zhaojie Zhu[a], Chaoyang Tu[a,*]

[a] Key Laboratory of Optoelectronic Materials Chemistry and Physics, Fujian Institute of Research on the Structure of Matter, Chinese Academy of Sciences, Fuzhou City, Fujian Province 350002, PR China

[b] University of Chinese Academy of Sciences, Beijing 100039, PR China

ARTICLE INFO

Keywords:
Crystal growth
Thermal properties
Optical properties
Energy transfer
Mid-infrared laser

ABSTRACT

Enhanced 2.86 μm emission corresponding to Ho^{3+}: $^5I_6 \rightarrow {}^5I_7$ was achieved in Nd^{3+}/Ho^{3+} codoped $CaLaGa_3O_7$ crystal for the first time. The detailed spectroscopic properties and energy transfer mechanism of the as-grown crystal were investigated. The results show that the Nd^{3+} ion is not only a very good sensitizer in a Ho^{3+} doped $CaLaGa_3O_7$ crystal, but also an appropriate deactivated ion with efficient depopulation of the Ho^{3+}: $^5I_7$ level for enhancing the 2.86 μm fluorescence emission. And the energy transfer efficiency of Ho^{3+}: $^5I_7 \rightarrow Nd^{3+}$: $^4I_{13/2}$ is estimated to be 93%, which indicates that the self-termination effect for the 2.86 μm holmium laser is suppressed successfully in Nd^{3+}/Ho^{3+}: $CaLaGa_3O_7$ crystal. Besides, the thermal properties of Nd^{3+}: $CaLaGa_3O_7$ crystal were also studied. In conclusion, the introduction of Nd^{3+} is favorable for achieving an enhanced 2.86 μm emission in Nd^{3+}/Ho^{3+}: $CaLaGa_3O_7$ crystal, which can act as a new promising candidate for mid-infrared lasers.

1. Introduction

Recently, novel mid-infrared (MIR) lasers with outputs around ~3.0 μm have attracted much attention for potential applications in remote sensing, countermeasures, imaging, eye-safe lidars, biomedical systems, and environmental agent detection [1–3]. Moreover, ~3.0 μm laser is also attractive as a pump source for MIR laser or optical parametric generation (OPG) laser system [4–6].

For crystalline MIR lasers, Ho^{3+} is an ideal luminescent center for achieving ~3.0 μm lasers through its $^5I_6 \rightarrow {}^5I_7$ transition, which has been extensively investigated [7–9]. However, there are two obstacles to prevent the Ho^{3+} activated ~3.0 μm lasers: one is that the intrinsic absorption of Ho^{3+} ions can't match the commercialized laser diodes (LDs) pumping wavelengths such as 980 or 808 nm. In order to solve this problem, a proper sensitizer ion with strong and broad absorption bands around 980 or 808 nm has usually been introduced, such as Tm^{3+} [10], Yb^{3+} [11], or Nd^{3+} [12]. The other main obstacle limiting the development of Ho^{3+} doped laser is the self-terminating "bottleneck" effect, which results from the much shorter lifetime of the laser upper level $^5I_6$ than the lower level $^5I_7$, and thus might cause the ~3.0 μm laser to terminate owing to the populations in upper level unable to relax to the lower level quickly. In order to over come this negative effect, one solution is to reduce the lifetime of the lower level $^5I_7$ of Ho^{3+} by codoping with deactivating ions. These ions can decrease the lower level populations of Ho^{3+}: $^5I_7$ effectively, which is beneficial for population inversion and thus lowers ~3.0 μm laser threshold and increases laser output power. Fortunately, Nd^{3+} is the only one able to act as sensitization and depopulation ions simultaneously [13], and then the two problems can be partly solved by Nd^{3+} codoping [14]. Nevertheless, there are few reports about the use of Nd^{3+} as a sensitizer and deactivator of Ho^{3+}, meanwhile for achieving an efficient 2.86 μm fluorescence emission.

Then Fig. 1 shows the energy level scheme of Nd^{3+} and Ho^{3+} in comparison to Er^{3+}. In the Nd^{3+}/Er^{3+} codoping system, though the ~3.0 μm laser operation on the self-terminating transition ($^4I_{11/2} \rightarrow {}^4I_{13/2}$) is inhibited [15,16], an up-conversion process also occurs under 808 nm LD excitation, which leads to a strong population of the excited state of erbium ion. However, up-conversion is less efficient in Ho^{3+} singly doped crystal and laser oscillation is less common under LD excitation of the Ho^{3+}: $^5I_6$ upper laser level [9]. Fortunately, in Ho^{3+} system, the above problems can be solved to a great degree by Nd^{3+} codoping. Under the excitation of a common 808 nm LD pump, the Nd^{3+} ion is excited to the excited state ($^4F_{5/2}$ + $^2H_{9/2}$) and, subsequently, decays nonradiatively to the $^4F_{3/2}$ level, and then transfers the excitation energy to Ho^{3+}: $^5I_5$, indicating that the Nd^{3+} can be used as a sensitizer ion of Ho^{3+}. After that, ions in the $^5I_5$ level decay nonradiatively to $^5I_6$, and then ions on the $^5I_6$ state decay radiatively to $^5I_7$ with 2.86 μm emission. Finally, ions in the $^5I_7$ level undergo an ET2 process to the $^4I_{13/2}$ level of Nd^{3+}, which depopulates ions on the Ho^{3+}: $^5I_7$ level, making the possibility of population inversion for

* Corresponding authors.
E-mail addresses: 1397054528@qq.com (Y. Liu), wy@fjirsm.ac.cn (Y. Wang), tcy@fjirsm.ac.cn (C. Tu).

https://doi.org/10.1016/j.jlumin.2018.04.050
Received 23 March 2018; Received in revised form 13 April 2018; Accepted 23 April 2018
Available online 24 April 2018

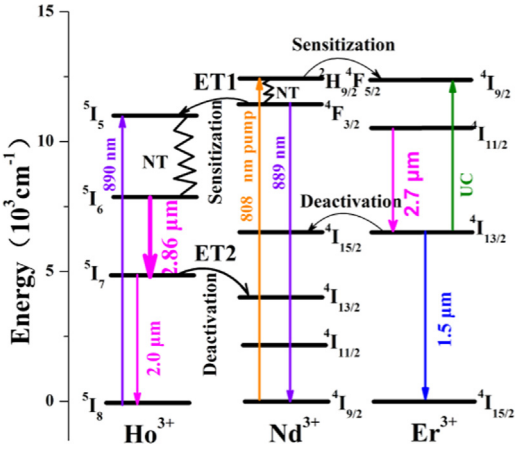

Fig. 1. Energy level scheme of Nd^{3+}, Ho^{3+} in comparison to Er^{3+}.(UC: up-conversion, NT: nonradiative transition, ET: energy transfer.).

Ho^{3+}: $^5I_6 \rightarrow {}^5I_7$.

To date, among the various matrix materials of mid-infrared solid-state lasers, lots of previous works have mainly paid attention to fluoride, aluminate and gallate crystals [12,13,17,18], due to their low phonon energy, high thermal stability, stable chemical durability and so on. In this work, $CaLaGa_3O_7$ (abbr. as CLGO) single crystal was chosen as the host matrix, because it has lower melting point (about 1600 °C) [19]. As compared with the above aluminate and gallate crystals, large sized crystals with high optical quality can be obtained more easily by using Czochralski (CZ) technique. To our knowledge, there has been no systematic study of the thermal properties of Nd^{3+}: CLGO crystal and the optical properties of Nd^{3+}/Ho^{3+}: CLGO crystal.

In this letter, we reported thermal properties of Nd^{3+}: CLGO crystal and the enhanced 2.86 μm emission in Nd^{3+}/Ho^{3+} codoped CLGO crystal for the first time.

2. Experimental details

The 2 at% Nd^{3+} and 1 at% Ho^{3+} codoped CLGO single crystal was grown by the CZ technique, 1 at% Ho^{3+} and 2 at% Nd^{3+} singly doped CLGO crystal were also grown in our pervious work [20,21]. 99.99% purity La_2O_3, Ho_2O_3, Nd_2O_3, Ga_2O_3 and $CaCO_3$ (A.R. grade) commercial powders weighed out according to the compositional formula, with an extra 1 wt% Ga_2O_3 to compensate Ga loss owing to its evaporation. The crystals' growth process was introduced in detail in our previous work [20,21]. Finally, a transparency Nd^{3+}/Ho^{3+}: CLGO crystal was obtained, as shown in Fig. 2(a), with the dimension of Φ 20 × 35 mm^2.

The XRD pattern of the grown Nd^{3+}/Ho^{3+}: CLGO crystal was studied by X-ray diffraction (Miniflex600), as it shown in Fig. 2(b). The diffraction peaks of the samples are well indexed to the standard Joint Committee on Powder Diffraction Standards (JCPDF) file [No. 39-1127] of CLGO crystal and there are no additional impurity peaks in the pattern, which indicates the formation of pure tetragonal phase of Nd^{3+}/Ho^{3+}: CLGO. The concentrations of Nd^{3+} and Ho^{3+} in the grown crystals were measured by inductively coupled plasma atomic emission spectrometry (ICP-AES) analysis. And the concentrations of Nd^{3+} and Ho^{3+} ions in Nd^{3+}/Ho^{3+}: CLGO crystal were measured to be 7.92×10^{19} ions cm^{-3} and 1.50×10^{19} ions cm^{-3}, respectively. The Ho^{3+} concentration in Ho^{3+}: CLGO crystal was measured to be 1.27×10^{19} ions cm^{-3}.

The absorption spectra was measured using a Perkin-Elmer UV–VIS–NIR Spectrometer (Lambda-900). The emission spectra and fluorescence lifetime were measured using an Edinburgh Instruments Fluorescence Spectrometer. Samples with dimensions of $3.0 \times 5.0 \times 0.9$ mm^3 were optically polished for spectral measurement. To obtain comparable results, the measurement conditions for each group of spectra were kept the same for two samples.

The thermal expansion of Nd^{3+}: CLGO was measured using a Diatometer 402 PC thermal–mechanical analyzer, over a temperature range of 200–800 K. The sample used for the thermal expansion measurement was processed into a rectangular piece of dimensions $40.0 \times 4.0 \times 6.20$ mm^3 along *c*-axis and $40.0 \times 4.0 \times 7.72$ mm^3 along the *a*-axis, respectively. The thermal expansion was measured by heating at 5 K/min. The thermal conductivity was measured by a LFA457 equiment. The samples were cut with dimensions of $10.0 \times 10.0 \times 2.0$ mm^3 along the *a*-axis and *c*-axis.

3. Results and discussion

3.1. Thermal properties

Fig. 3 shows the temperature dependence of the thermal conductivity of Nd^{3+}: CLGO along the *a* and *c*-axis, which was determined by using the formula $\kappa = \lambda \rho C_P$, where λ is the thermal diffusivity coefficient, ρ is the measured density, and C_P is the specific heat. The thermal conductivity along the *a*-axis increases from 1.401 to 1.791 W m^{-1} K^{-1} over the temperature range from 297.6 to 624.1 K; Along the *c*-axis, it increases from 1.189 to 1.588 W m^{-1} K^{-1} over the temperature range from 296.8 to 624.2 K, which is smaller than that of Nd: $SrLaGa_3O_7$ crystal [22]. The thermal conductivity of Nd^{3+}: CLGO increases with the increment of temperature, which shows glass-like behavior, owing to the possible effects of the disordered structure [23].

The thermal expansion ration versus temperature of Nd^{3+}: CLGO crystal is shown in Fig. 4. From the plot, it can be seen that the thermal expansion along the *a* and *c*-axis is almost linear within the temperature range from 200 to 800 K. The average linear thermal expansion coefficients along the *a*- and *c*-axis were calculated to be 8.32×10^{-6}/K and 7.00×10^{-6}/K, respectively, which is larger than that of Nd: $SrLaGa_3O_7$ crystal [22]. A small difference between the thermal expansion coefficient components along the *a*- and *c*-axes is favorable for

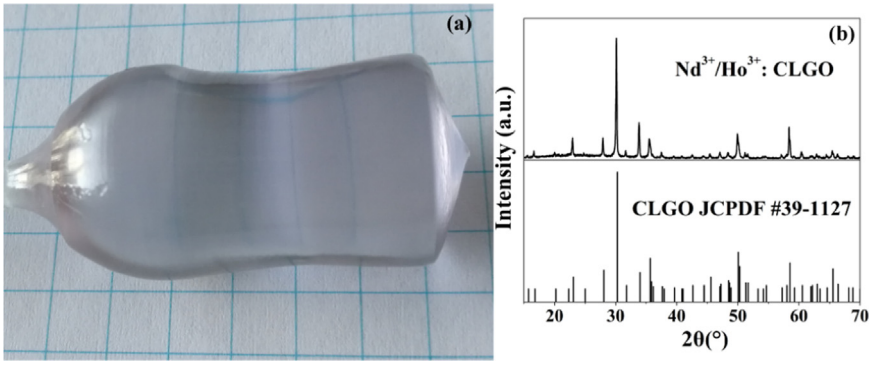

Fig. 2. (a) The photograph and (b) X-ray diffraction patterns of the grown crystal Nd^{3+}/Ho^{3+}: CLGO.